

## Assessment of Bouguer Gravity Anomaly over Part of Chad Basin North Eastern Nigeria,

Sulaiman Garba Yana<sup>1,2</sup>, Juzhi Deng<sup>1,2</sup>, Hui Chen<sup>1,2</sup>, Yanguo Wang<sup>1,2</sup>

<sup>1</sup> State Key Laboratory of Nuclear Resources and Environment, East China University of Technology, Nanchang, Jiangxi Province, China, 330013

<sup>2</sup> School of Geophysics and Measurement-control Technology, East China University of Technology, Nanchang Jiangxi Province, China, 330013

### ABSTRACT

Using Bouguer gravity data, processing and interpretation of structural features covering the Chad basin were performed. Since knowledge about the structural makeup of the subsurface geology within the study area is of great importance considering the fact that the area is economically feasible in terms of hydrocarbon and mineral exploration, detailed filtering techniques like the vertical derivatives, horizontal derivatives, upward and downward continuation were carried upon the residual using the oasis montaj and surfer 16 software. The residual, which is a true reflection of short wavelength anomalies arising from shallower geological structures, was however acquired through regional-residual separation by subtracting upward continued data at 5000m. Low and high amplitude/gravity anomalies were modeled from the Bouguer gravity anomaly map. These anomalies have a tectonic trend of E-W, ENE to NE, WNW, and NW directions. These trends are structural and tectonic indicators. As evidenced by the structural/tectonic trend, the general pattern of the gravity signatures obtained extremely corresponded to the well-known geology of the Chad basin region. Forward and Inverse modelling methods were used in the quantitative interpretation with the aim of determining depth to the gravity source bodies, gravity density, and the possible mineralization in the study area. The estimated depths from the forward and inverse modelling methods for profiles 1-7 are 3446, 6921, 6182, 5199, 3321, 3152, and 2762m respectively. The respective density values were 0.182, 0.098, 0.043, 0.091, 0.108, 0.079 and 0.079 gmcc<sup>-1</sup>, which indicate the presence of sedimentary intrusions (basalt or limestone), few metamorphic rocks (schist) and minerals (magnetite).

**Keywords:** Bouguer gravity anomalies, densities, Basement, modelling, residual, sediments,

Date of Submission: 25-05-2021

Date of Acceptance: 08-06-2021

### I. INTRODUCTION

The Earth's subsurface contains natural resources, which include hydrocarbon, mineral deposits, rocks, underground water, and so on [1]. Over the years, the search for subsurface natural resources especially mineral deposits and hydrocarbon potential has become a major concern to geologists, geophysicists, and exploration scientists. A large portion of the country's revenue comes from the export and domestic sale of petroleum and minerals deposits. Many geophysical explorations have been executed in the Niger Delta region of Nigeria, hence the fear that soon or later the economic reserve of the country from such area may have hitch due to depletion in the hydrocarbon potentials and mineral deposits. Therefore, the need to investigate the economic minerals and hydrocarbon potentials of other geologic provinces, especially in Chad Basin which is one of the inland Basins in Nigeria presumed to have a high level of

hydrocarbon potential apart from other Earth minerals with a high level of economic values.

There is the probability that hydrocarbon potential and other economic mineral deposit might be found in the Chad Basin following the discoveries of hydrocarbon potentials and other mineral deposits in the neighboring countries such as the Republic of Niger, Chad, Sudan, and Libya which have a similar geological structural setting as that of the Chad Basin. In addition, the possession of the Chad Basin of some favorable features such as the age of the Basin, thickness of structurally related trap which encourages the accumulation of hydrocarbon potential and mineral deposits call for its geophysical investigation, [2]. Furthermore, the order by the federal government of Nigeria that national petroleum cooperation (NNPC) should resume exploration activities in the Chad Basin, triggered off the interest to investigate this sedimentary Basin, [3]. Some researchers have

executed depth to basement estimation using source parameter imaging in other areas of the Basin, [4]. In addition, these researches were executed using aeromagnetic data of 1974 and 1980. Additionally, some of the works were executed using land survey measurement, which could be limited in some regions due to differences in topography, thus not giving enough details of the area.

Consequently, there is a need to utilize high-resolution airborne data which will not only dispense the capability of traversing areas that were otherwise difficult to cover by land survey geophysical techniques, but will generate a much more precise and better-resolved picture of the geologic structures in the region. It is a well-known fact that the Chad basin is very complex, and it carries high economic value. In view of this, numerous geophysical techniques have been used by geophysicists, geologists, or earth scientists to work out the subsurface geology of the Chad basin region. Most of the previous studies cover the whole portion or some parts of the area under investigation in this study. Nevertheless, there is a fewness of information as regards the use of Bouguer gravity data in studying the structural composition/complexity of the Chad basin. Hence to fill that lacuna, this research tried to investigate the subsurface geology by delineating structural features and mineral deposits in the region. This was accomplished by interpreting and correlating the gravity anomalies with the geology of the study area.

Therefore, the result from the work could be used to suggest portions of mineral presence in the area as well as the possible depths of assessment.

## II. GEOLOGY OF THE STUDY AREA

The research area is located in the Nigerian sector of Chad Basin. The Chad basin lies within latitude  $11^{\circ}\text{N}$  and  $14^{\circ}\text{N}$  North and longitude  $9^{\circ}\text{E}$  to  $14^{\circ}\text{E}$  (Figure 1). It lies within a vast area of central and West Africa at an elevation between 200 and 500m above sea level and covers approximately  $230,000\text{ km}^2$ , [5]. It is the largest area of inland drainage in Africa, [6]. It stretches into portions of the republic of Niger, Chad, Cameroon, Nigeria, and Central Africa. The Nigerian sector of Chad Basin is about one-tenth of the basin and has a broad-ranging sediment-filled depression spanning northeastern Nigeria and adjoining parts of the Republic of Chad.

The area generally is endowed with rock mineral base resources such as clay, salt, limestone, kaolin, iron ore, uranium, mica, etc, [7]. Therefore, the sedimentary rocks of the study area have a cumulative thickness of over 3.6 km, and the rocks comprised of a thick basal continental sequence overlaid by transitional beds followed by a thick succession of quaternary Limnic, fluvatile and eolian sand, clay, etc, [8]. The stratigraphic sequence shows that Chad, Kerri-Kerri, and Gombe formations have an average thickness of 130 to 400m. Beneath these formations are the Fika shale with a dark grey to black in colour, with a total average thickness of 430m. Others are Gongila and Bima formations have the total average thicknesses of 320 and 3500m, respectively, [9].

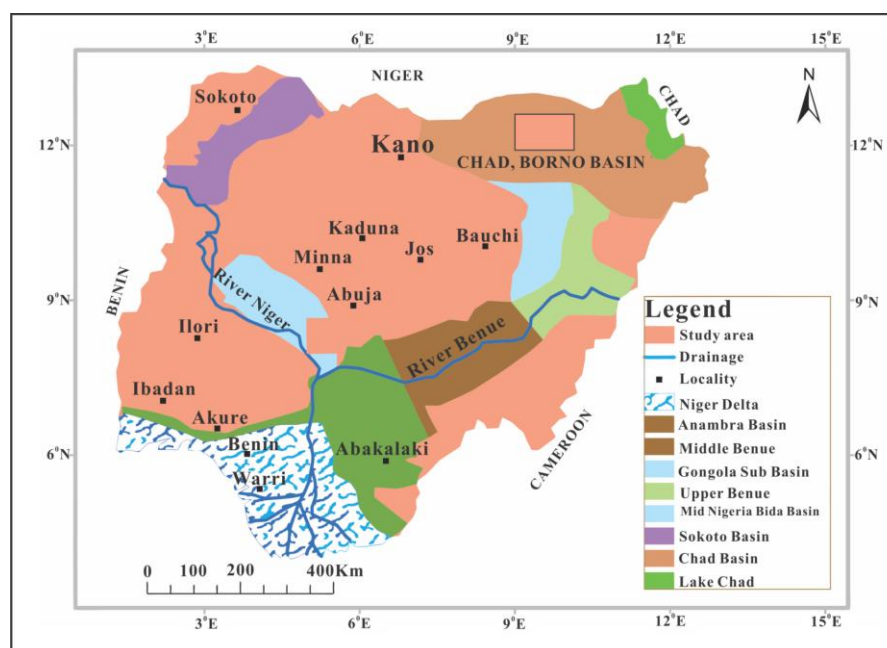
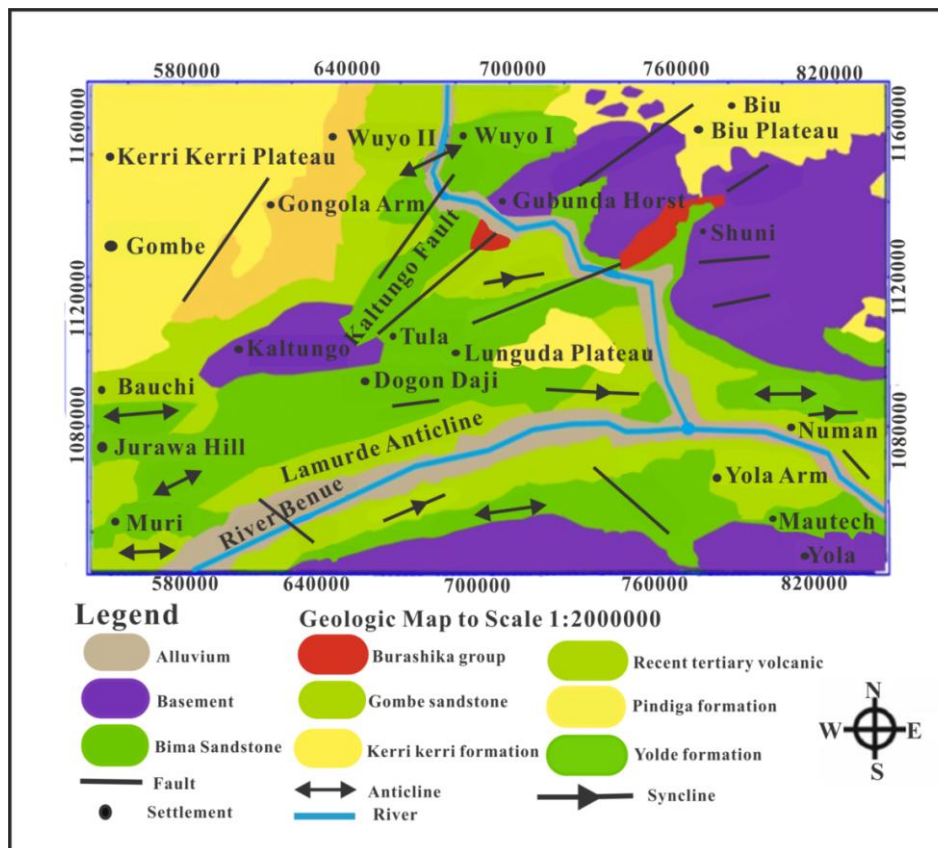


Figure 1: The Map of Nigeria Showing the Location of Chad Basin. [10]



**Figure 2:** Geological map of the study area (The Nigerian Geological Survey Agency, NGSA, Abuja)

### III. MATERIALS AND METHODS

Digitized Bouguer gravity data covering the study area was utilized for this research. The Bouguer gravity data were acquired from the Nigerian Geological Survey Agency, NGSA, in half degree sheet and in Geosoft file format. The Oasis Montaj Modeling software and surfer 16 software was used for processing, analysis, and interpretation.

For the research, the qualitative and quantitative method was implemented on the Bouguer gravity data. By the qualitative method, regional-residual separation was applied on the Bouguer data so as to prevent the influence of unwanted deep-seated regional's on the significant shallow seated residuals. Furthermore, filtering was

then applied on the residual data and as a result, other qualitative maps like the first vertical derivative, first horizontal derivative, upward continuation, and the downward continuation maps were generated. Consequently, visual inspection and correlation of the various maps with the subsurface geology were executed. The tectonics of the study area was carefully investigated by analyzing the structural trends of the maps. Analysis was performed on the map on the basis of amplitude of the anomalies and identification of anomalous boundaries, volcanic zones, lineaments, folds, faults, dykes, seals, and other regional structures that, perhaps, help in hydrocarbon and other mineralized fluid migration and entrapment.

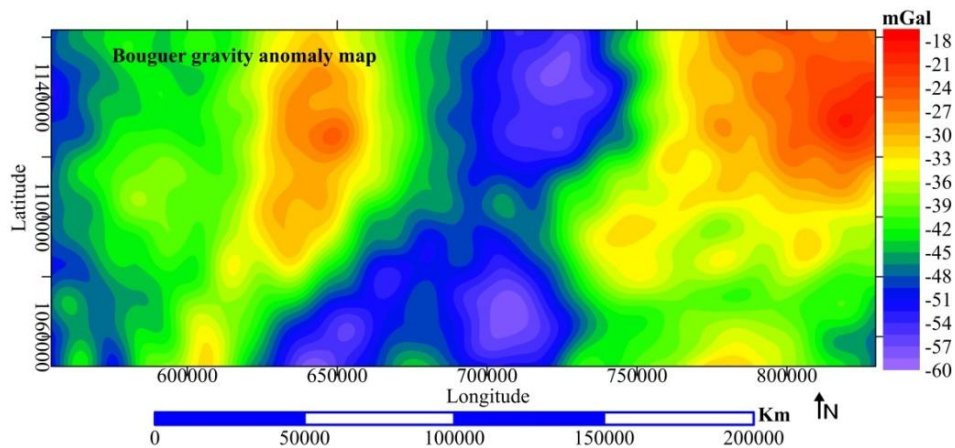


**Figure 3:** Bouguer gravity map of the study area (mgal)

The colours on the Bouguer gravity map vary from red and yellow at the northeast and northwestern part of the map, the north-southern and western edge of the map dominated by blue colour. The colour contrasts reflect the summation of the gravitational effect of all subsurface rocks within the study area and as such horizontal variations of rock densities are revealed. The blue and green colours found at the north-south and the western parts of the map are associated with possible rocks with low density-values. Contrarily, high gravity values apparently dominate the northeast and northwestern part of the map. It can therefore be deduced that higher density rocks and/or structures occur at the northeast and northwestern part of the study area while low-density rocks and/or structures are seen at the north southern portion of the map. Therefore, this is a clear indication of dense rocks decreasing northeast and northwards within the study area. [11]

stated that the northeast and northwards decrease of rock densities usually observed in Bouguer gravity maps may indicate that the crust-mantle boundary is deeper within the northeast and northwards than the north-south and western edge. [12] suggested that such a decrease in gravity represents the increasing thickness of the continental crust. According to [13], gravity high regions are associated with basement rocks while gravity low regions are associated with sedimentary rocks. Nevertheless, the grid map disclosed big-scale negative Bouguer anomalies trending Southwest-northeast to east-west over the central part of the study area. The appearance of linear patterns and prominent steep gradients on previous locations may be suggesting the existence of major basement fault lines. The close negative anomaly may be connected to sedimentary basins and/or grabens.

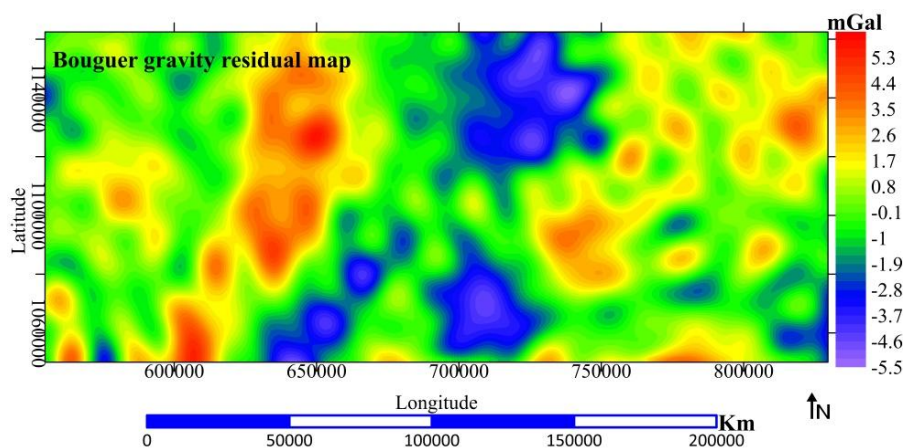


**Figure 4:** Residual Bouguer gravity map (mgal)

The residual map (Figure 4) shows random and smoothed gravity anomalies with gravimetric values ranging from -5.5 mgal to -0.1 mgal for low gravity regions and 0.8 mgal to 5.3 mgal for high

gravity regions. Two distinct gravity lows exist within the study area; they are the gravity low with blue colouration and that with green colouration. Gravity low indicated by the blue colours is located

within the north, west, south, and southeastern part of the map while the gravity low expressed by the green colour is entirely distributed within the study area. The colour variation could be a result of weathering of gravimetric rock units involved. Anomalies with high gravity values are noticeable at the eastern, northwestern, central, southeast, and southwestern portion of the map. [14] opined that the gravity highs are associated with basement rocks like migmatite and granite while the gravity lows are due to sedimentary rocks like shale, sandstone, and/or limestone. The residual map highlights varying degrees of contours that are closely packed. The closeness of the contour can be related to shallow related gravity bodies. These contours vary from being circular, elliptical to being elongated

linear contours. At the southeastern portion of the map, closely packed and elongated linear contours with low relief are conspicuous. These linear elongated contours form the fault belt zone. [15] believe that this anomalous pattern results from subsurface faulting that has displaced gravimetric rocks. The elongation of the contour depicts faults that serve as conduits for economic deposits while the closeness of the contours shows that the faults are of shallow origin. Hence, faults of shallow origin exist within the study area. Nevertheless, the contour architecture found in the residual is quite different from the contours observed in the Bouguer gravity. This is attributed to the regional-residual separation performed on the Bouguer map.

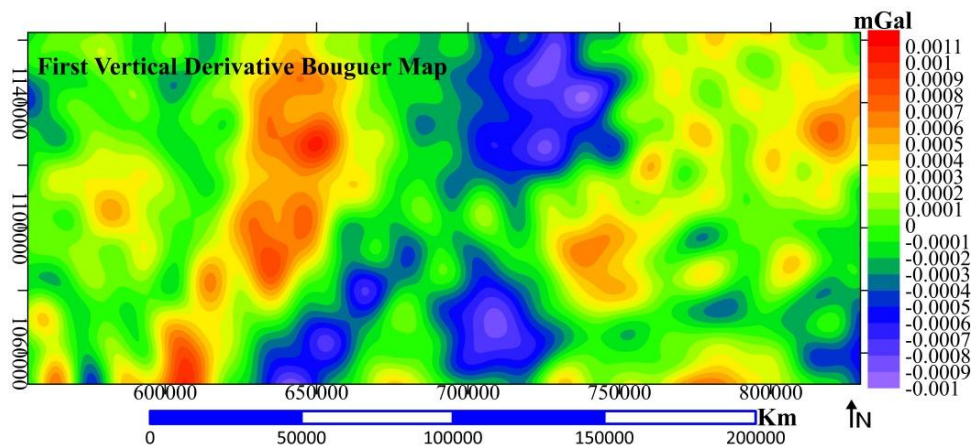


**Figure 5:** First Vertical Derivative Bouguer Map (mgal)

The colour map variations highlighting shallow seated gravity bodies are illustrated in the first vertical derivative map (Figure 5). Unlike the residual gravimetric sources, the gravity values are too small value. However, anomalous bodies with high and low density are still distinguishable. Sources with high gravity values ranging from 0.0001 mgal to 0.0011mgal can be seen occurring at the eastern, northwestern, and western side of the map while low values ranging from -0.001mgal to -0.0001mgal. The 0.000 mgal value is a zone with no vertical gravity contrast. The high gravity anomaly existing at the northwestern portion is similar to the high gravity anomaly which occurred at the same region in the same Bouguer residual map. The anomaly runs towards the southwestern and northern portions. Gravity lows emerging clearly on the

Bouguer residual map are unnoticeable on the first vertical derivative map. This is owned by the fact that the one-dimensional fast Fourier transform - the first vertical derivative filter- recognizes some of the low gravity values as artifacts. Unlike the Bouguer residual map, localized and shorter wavelength contours are noticeable. Dominating on the map are closed gravity contours. The shorter wavelength contours are indication that shallower gravity sources are accentuated using the first vertical derivative filter. Embedded inside high gravity contours occurring across the map are contours of higher gravity values. According to [16], the higher gravitational values that are embedded are distinct lithology from the surrounding. Existent on the map are E-W, N-S, ENE-WSW, and WNW- ESE tectonic trends.

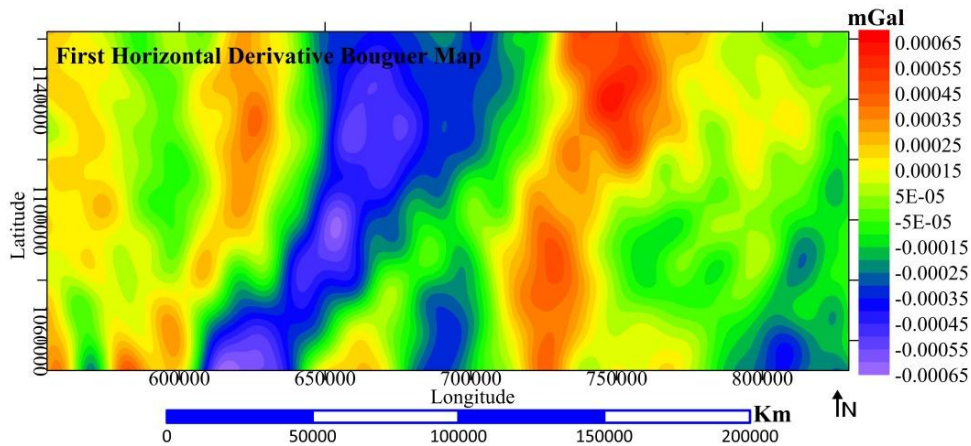


**Figure 6:** First Horizontal bouguer gravity map (mgal)

The horizontal derivative map (Figure 6) delineates acute preponderate high gravity field changes. Gravity sources with large areal extent are visible running from the north to the southern region of the map. [17] stated that sources with such a large area extent can be attributed to the homogeneity of the source. They also stated that such anomalous feature is produced by large density contrast. Gravity lows can be seen more at the extreme northern

portion to the southern portion of the map. Minor circular gravity lows are also noticeable towards the southeastern zone of the map. E-W and N-S tectonic trends are visible on the map but with the former occurring frequently. Dominate N-S directional trend is an indication of less noise within the map. Gravity anomalies within the map have values ranging from 0.00065 mgal to - 0.00065mgal.

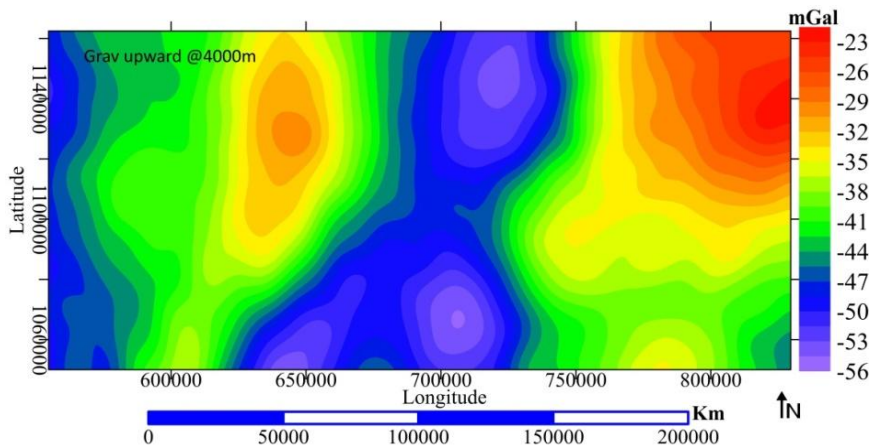


**Figure 7:** Upward Continued Bouguer Gravity Map at 4000m (mgal)

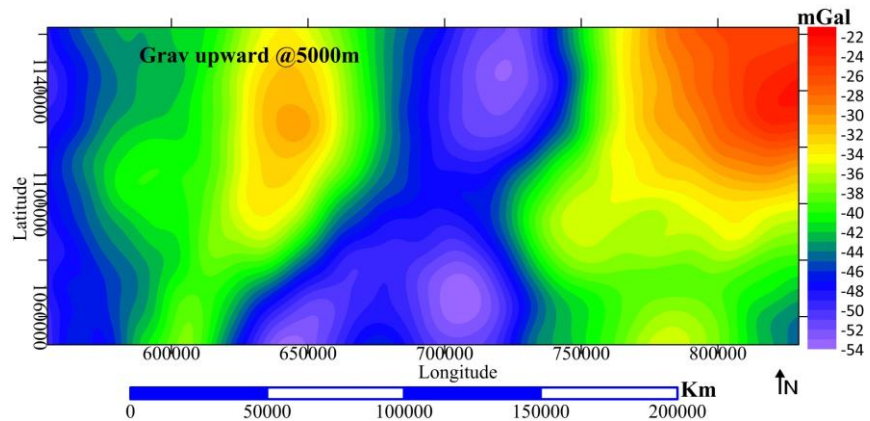


**Figure 8:** Upward Continued Bouguer Gravity Map at 5000m (mgal)

The upward continuation map at 4000m (Figure 7) highlights smoothed anomalies that are a true reflection of basement features. The anomalies found when the measurement point was 4000m away from the source are almost similar to that observed on the residual map. They are dissimilar in the nature of the anomalies found around the northwestern and northeastern parts of the study area.

The gravity highs appearing at the extreme eastern part of the upward continuation map are sharpened with their edges pointing upwards. Moving upwards, the structural or gravity lows adjacent to the gravity highs are more pronounced. A slight difference exists between the upward continuation map and the residual Bouguer gravity map. Closed circular and elliptical gravity contours, which are absent on the residual map, are visible at

the north, and south of the upward continued map at 4000m. Gravity signatures trending in the N-S, and ENE-WSW direction are visible on the map.

Prominent on the upward continuation map at 5000m (Figure 8) are structural highs depicting gravimetric sources with high-density contrast. A similar type of gravity anomaly with high-density contrast is observed both on the upward continuation map at 5000m and the residual map. Slight changes can be seen at the Northeast, eastern, southeastern and western edges of both maps. At the southwestern portion of both maps, isolated and alternating gravity high and low which is discernible on the residual is absent on the upward continuation map at 5000m. Isolated circular anomalies which are not present on the upward continuation map at 5000m can be identified at the extreme northern portion of the residual Bouguer map.

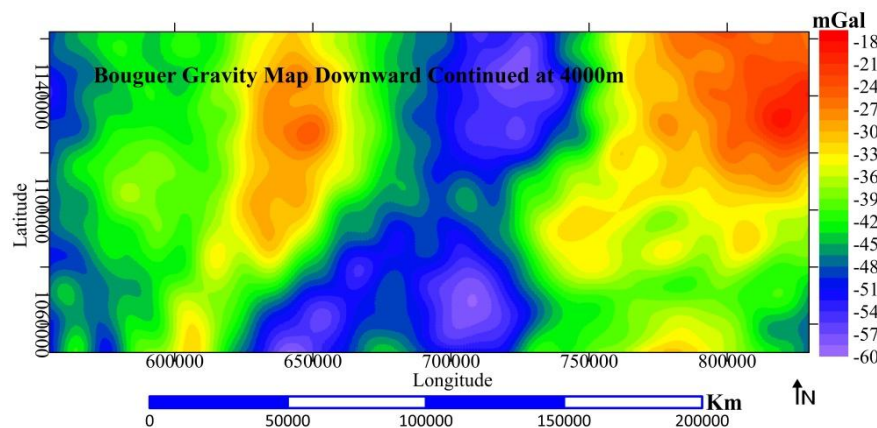
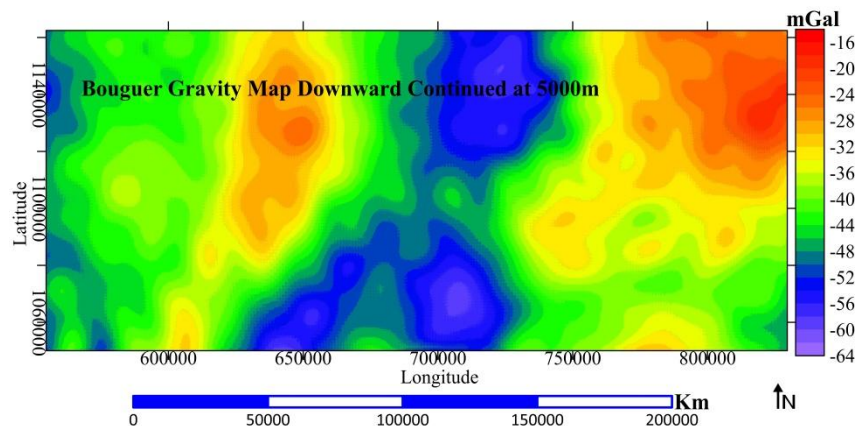


Figure 9: Bouguer Gravity Map Downward Continued at 4000m (mgal)

High and low gravity values are obvious when the measurement point was downward continued at 4000m (Figure 9). However, gravity sources with high values occur frequently within the map. The anomalous sources with high gravity sources can be seen in a similar position with the high gravity sources found on the upward continuation and residual maps. But on the downward continuation map, the dense sources with high values are of shorter wavelength and less broadened. The shorter wavelength and less broadening nature of the gravity anomalies is a reflection of shallow related gravity sources. Low gravity sources with short and relatively long wavelengths can be seen at the northern, north-south, western edge, and southeastern regions of the map. Isolated, circular, and elliptical gravity contours are noticeable on the downward

continuation map. N- S dense gravity signatures are seen visibly at the eastern portion of the map. Moving towards the western portion of the map are gravity contours trending in the N-S and NW-SE directions.

Few gravity anomalies can be seen having a trend of NE-SW, N-S, E-W, and NW-SE directions at the western, northwestern, and southwestern portion of the map. It is pertinent to know that the elongated structural linear trends which appeared at the north-south region of the residual map, upward continuation maps at 4000m and 5000m, and downward continuation maps at 5000m and 4000m, are visible on the downward continuation map at 5000m. This consistency can therefore help in inferring that there is an existence of fault zone at the north southern region of the study area.



**Figure 10:** Bouguer Gravity Contour Map Downward Continued at 5000m (mgal)

The residual map, upward continuation maps at 4000m and 5000m and the downward continuation maps at 4000m and 5000m, colour contrasts are apparently seen. Similar types of gravity highs and lows occur in both the residual and downward continuation maps at 5000m. This implies that shallow related sources can be delineated using downward continuation filter at 5000m, therefore as a result gravity bodies of similar configuration can be detected even when the measurement point is taken 5000m towards the gravity sources. Unlike the downward continuation at 4000m, sources with high gravity values are broadened at the eastern region of the map. This broad nature can be attributed to huge density contrast at that measurement point of the study area. On the downward continuation map, the goodness of the gravity lows seen on the Bouguer residual map structural low is maintained.

#### IV. GEOPHYSICAL MODELLING AND INVERSION USING POTENT

Some of the depths to basement techniques, such as local spectra, suffer from several setbacks in that they cannot accurately map the undulation in the basement as they give only the average depths [18]. Therefore, the need to construct forward gravity models that accurately represent basement topography cannot be over-emphasized. Thus, to confirm the strike, plunge, dip, and depth to basement block surfaces, to delineate the basement tectonic framework in the area under investigation,

seven profiles were modelled for the gravity grid. These profiles were taken in directions orthogonal to the prominent trends/structures and to cut across gravity aureoles. These profiles were traced out from the Bouguer gravity grid.

These traced out profiles were used as the observed profiles for 2 – dimensional modelling on Potent which is an extension of Oasis montaj software. These profiles' data retained the long wavelengths of the signal corresponding to deep-seated sources and suppressed the short wavelengths components indicating shallow sources. The anomalies were modelled using the foreknowledge of the geology of the study area and the depths to the basement were interactively modified to reduce error and achieve the best fit.

Interpretation of gravity field data using potent starts with observation of the image of the observed data, this is done by taken profiles on the field image. The associated subsets are automatically created by potent and displayed in a profile window. The model is consistent with observed physical values if its calculated field matches the observed values to some degree of precision. This is assessed by calculating the gravity field intensity due to the model and comparing it with the observed fields. Therefore, for this study seven profiles were taken on the gravity grid of (Figure 11) at **P1, P2, P3, P4, P5, P6,** and **P7**, which were modelled using potent software. Forward and inverse modelling methods conducted on those locations. Table 1 gives the summary of the result of the modeling process.

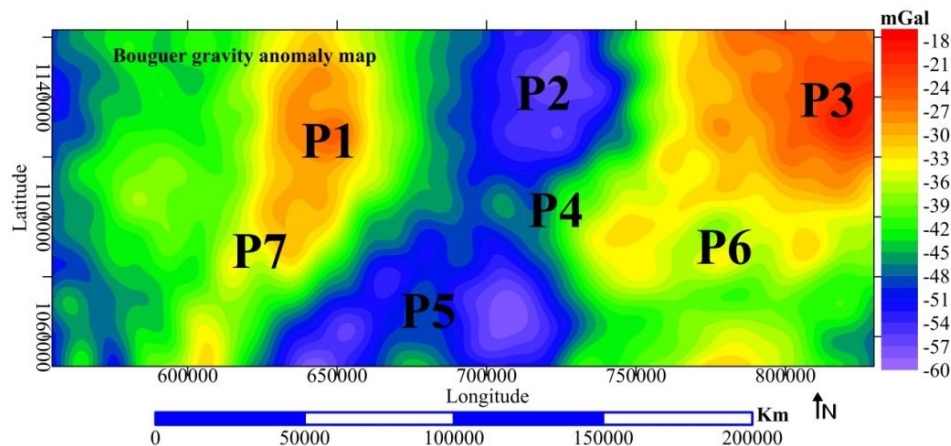


Figure 11: Bouguer gravity grid showing the locations of seven profiles

#### 4.1 MODELED GRAVITY PROFILE P1

P1 is a profile taken in the northwestern part of the research area. The model parameters are shown in Figure 12. During the forward and inverse modeling using an ellipsoid geometrical body (that is by adjusting the background, shape, position, and other properties of the geometrical body), a good mutual or complementary relationship between the

observed (blue) and calculated (red) field was achieved with the root mean square R.M.S difference of 0.0443% indicating a good model. The model revealed the gravity source at depth Z of 3446m, 6206m, and 5866m with density values of 0.182, 0.146, and 0.312gmcc<sup>-1</sup>. [19], [20] suggested that the density value corresponds to basalt rock material.

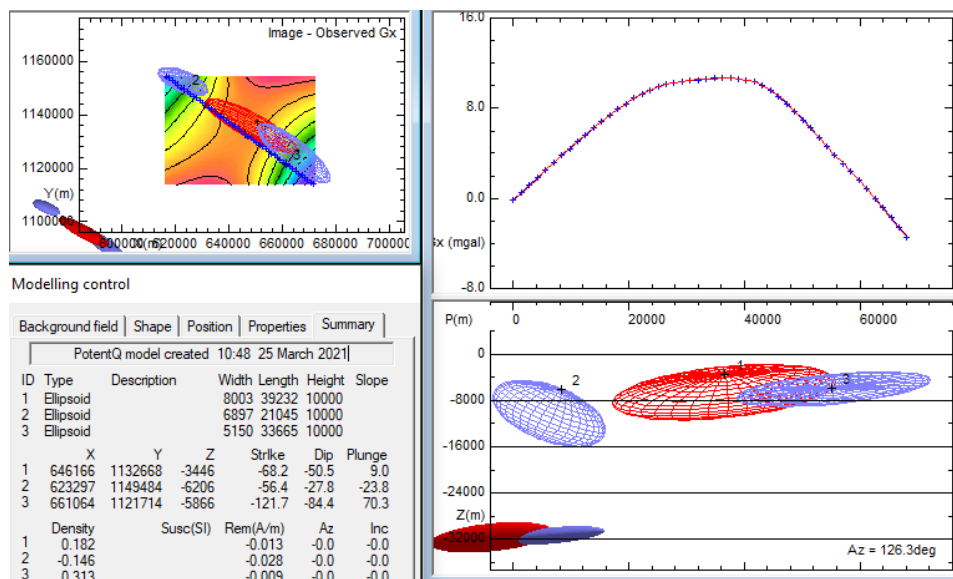


Figure 12: Profile 1 with R.m.s difference = 0.043%

#### 4.2 MODELLED GRAVITY PROFILE P2

Another profile was taken in the location marked P2 on the grid, within the northern region of the study area. The detail of forward and inverse modelling method conducted on P2 is given in Figure 13 and the model revealed gravity source at

depth Z of 6921m, 4149m, and 3954m with the R.M.S difference of 0.047% was used and a density values of 0.089, 0.017, and 0.193gmcc<sup>-1</sup> which corresponds to limestone and sandstone was obtained. The mineral group associated with these rocks includes gypsum and calcite.

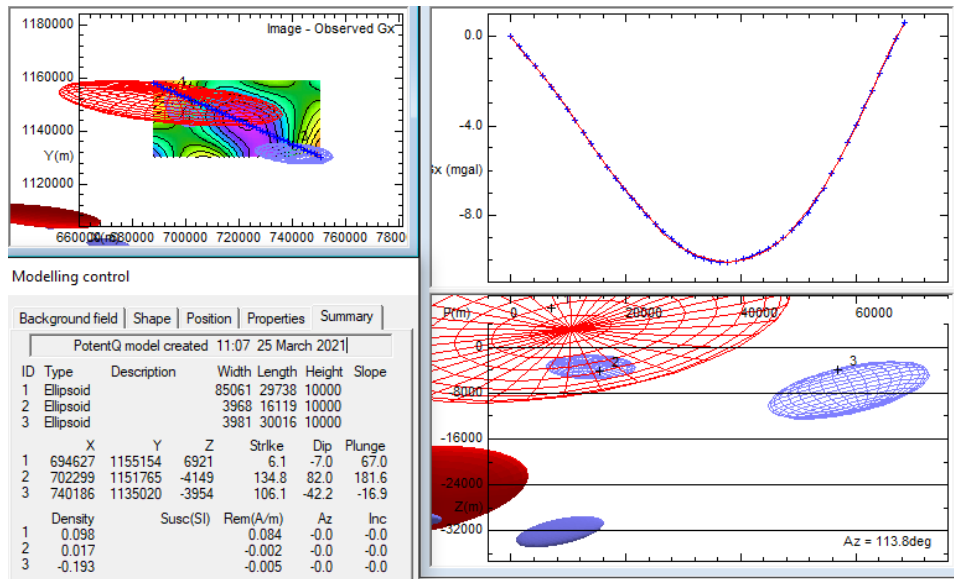


Figure 13: Profile 2 with R.m.s difference = 0.047%

#### 4.3 MODELLED GRAVITY PROFILE P3

Profile P3 was taken from the eastern part of the study area was also examined using an ellipsoid geometric shape for the model since it gives a better result than other geometric bodies such as sphere and rectangular prism. Figure 14 gives P3

modelled summary results with depth to gravity source depths Z of 6182m, 1260m, and 6363m with root means square (R.M.S) difference of 0.019% and density values of 0.043, 0.061, and 0.009gmcc<sup>-1</sup>. Therefore, the density values correspond to the sedimentary rock material [21].

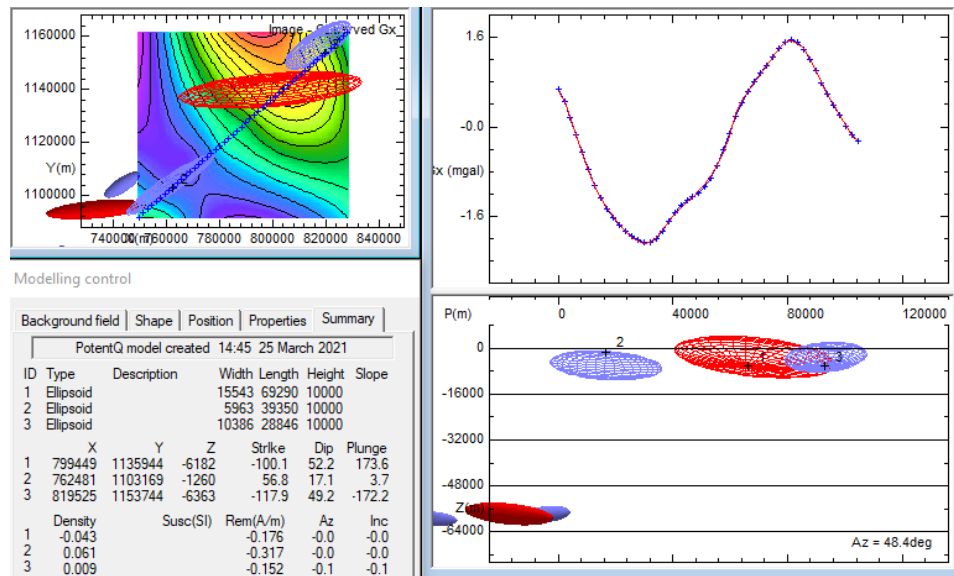


Figure 14: Profile 3 with R.m.s difference = 0.019%

#### 4.4 MODELLED GRAVITY PROFILE P4

Profile P4 was taken in the central part of the grid of the study area. The detail of the forward and inverse modelling method conducted on P4 is given in Figure 15 and the model revealed a depth to gravity source Z of 5199m, 5922, and 6445 with

R.M.S difference of 0.020% with density values of 0.091, 0.237, and 0.066gmcc<sup>-1</sup> which corresponds to limestone and sandstone source. The mineral group associated with these rocks includes gypsum and calcite.

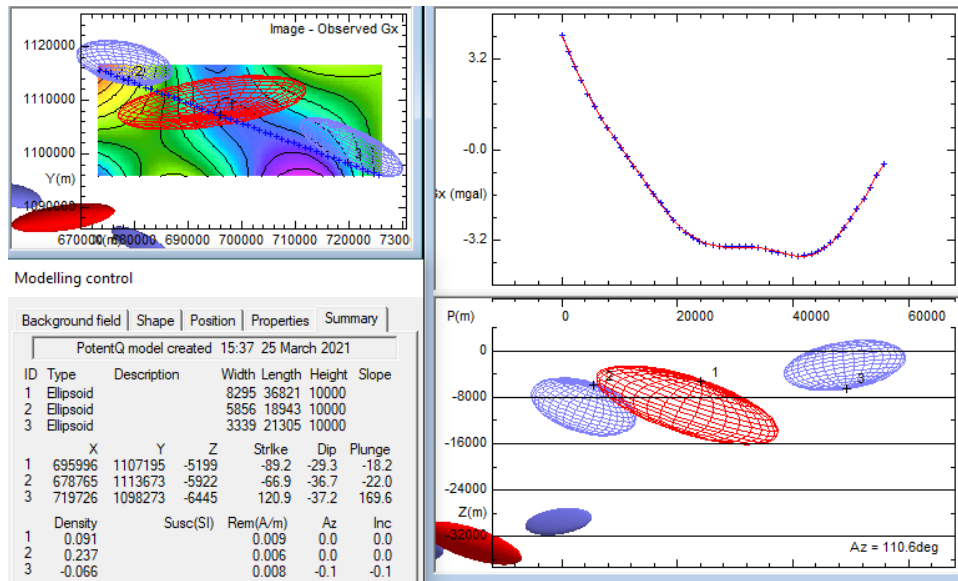


Figure 15: Profile 4 with R.m.s difference = 0.020%

#### 4.5 MODELLED GRAVITY PROFILE P5

P5 is a profile drawn in the southern region of the research area. The model parameters are shown in Figure 16. During the forward and inverse modeling using an ellipsoid geometrical body (that is by adjusting the background, shape, position, and other properties of the geometrical body), a good mutual or complementary relationship between the

observed (blue) and calculated (red) field was achieved with R.M.S difference of 0.033% indicating a good model. The model showed depths to gravity source Z of 3321m, 5802m, and 3876 with density values of 0.0108, 0.155, and 0.133gmcc<sup>-1</sup> which suggests that the density values corresponds to calcite or quartz, [19],[ 20].

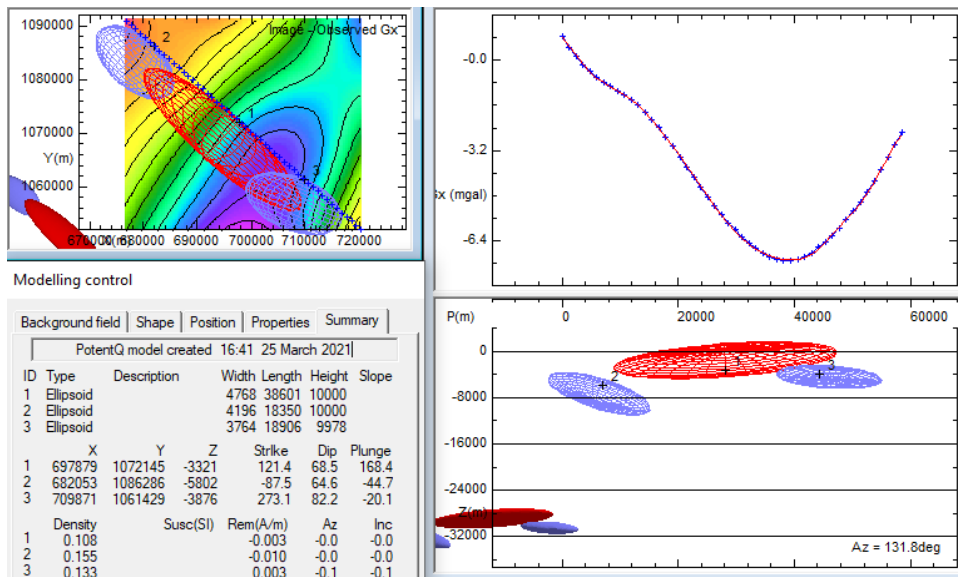


Figure 16: Profile 5 with R.m.s difference = 0.033%

#### 4.6 MODELLED GRAVITY PROFILE P6

P6 is a profile drawn in the southeastern region of the research area. The model parameters are shown in Figure 17. During the forward and inverse modeling using an ellipsoid geometrical body (that is by adjusting the background, shape,

position, and other properties of the geometrical body), a good mutual or complementary relationship between the observed (blue) and calculated (red) field was achieved with root mean square (R.M.S) difference of 0.013% indicating a good model. The model revealed gravity source at depths Z of 3152m,

603m, and 4619m with density values of 0.020, 0.022, and 0.043gmcc<sup>-1</sup> which corresponds with

basalt rock material [19],[20].

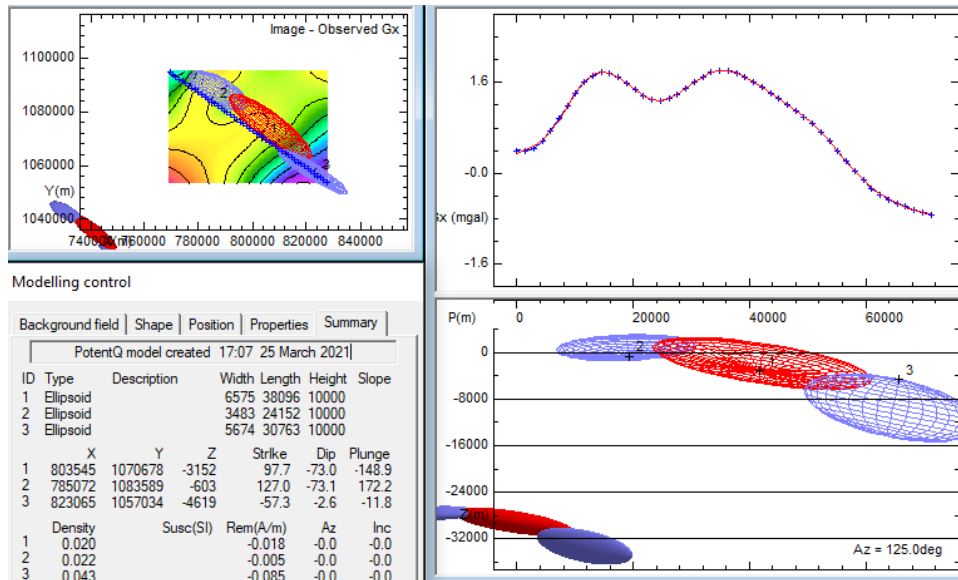


Figure 17: Profile 6 with R.m.s difference = 0.013%

#### 4.7 MODELLED GRAVITY PROFILE P7

And lastly, profile P7 is taken at the extreme western part of the study area. The model parameters are shown in Figure 18. In the process of the forward and inverse modelling using an ellipsoid geometrically body, a good mutual or complementary relationship between the observed and calculated field was achieved with a root mean

square (R.M.S) difference of 0.034%. The model revealed a gravity source at depths Z of 2762m, 7819m, and 390m with density values of 0.079, 0.116, and 0.080gmcc<sup>-1</sup> which corresponds to limestone and sandstones. The mineral group associated with these rocks includes bismuth and pyrite.

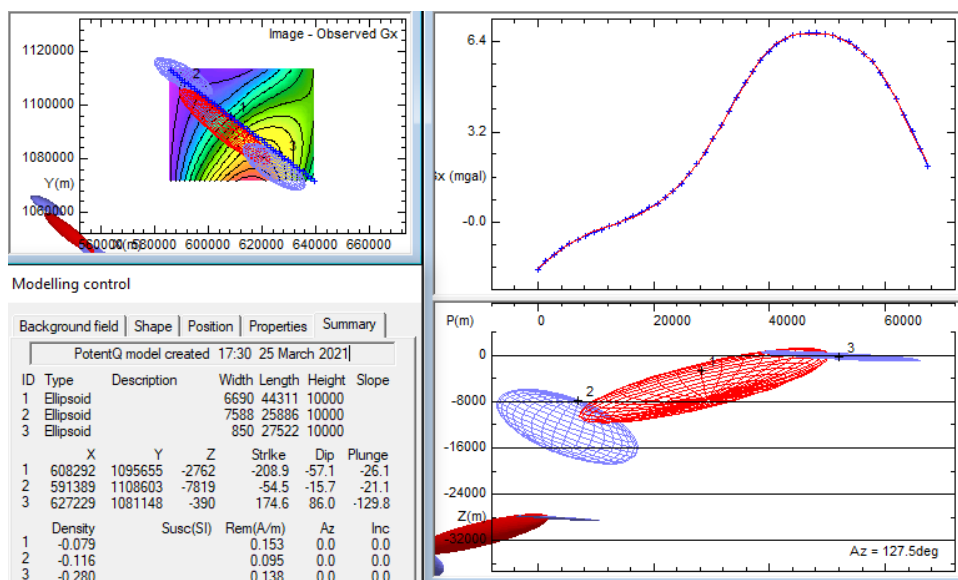


Figure 18: Profile 7 with R.m.s difference = 0.034%

**Table 1:** Summary of the forward and inverse modelling results of gravity data

Model gravity	Depth (M)	Dip (Deg)	Plunge (Deg)	Strike (Deg)	Body Shape	Density Value (gmcc <sup>-1</sup> )	Possible Minerals
1	3446	-50.50	9.00	-68.20	Ellipsoid	0.182	Basalt
	6206	-27.80	-23.80	-56.40		0.146	
	5866	-84.40	70.00	-121.70		0.313	
2	6921	-7.00	67.00	6.10	Ellipsoid	0.098	Pyrite
	4149	82.00	181.60	134.80		0.017	
	3954	-42.20	-16.90	106.10		0.193	
3	6182	52.20	173.60	-100.10	Ellipsoid	0.043	Calcite
	1260	17.10	3.70	56.80		0.061	
	6363	49.20	-172.2	-117.90		0.009	
4	5199	-29.20	-18.20	-89.20	Ellipsoid	0.091	Pyrite
	5922	-36.70	-22.00	-66.90		0.237	
	6445	-37.20	169.60	120.90		0.066	
5	3321	68.50	168.40	121.40	Ellipsoid	0.108	Pyrite
	5802	64.6	-44.70	-87.50		0.155	
	3876	82.20	-20.10	273.10		0.133	
6	3152	-73.00	-148.90	97.70	Ellipsoid	0.020	Limestone/shale
	603	-73.10	172.20	127.00		0.022	
	4619	-2.60	-11.80	-57.30		0.043	
7	2762	-57.10	-26.10	-208.90	Ellipsoid	0.079	Basalt
	7819	-15.70	-21.10	-54.50		0.116	
	390	86.00	-129.80	174.60		0.280	

## V. DISCUSSION

The Bouguer gravity anomaly map covering the research area was produced. The colour variations depicting low and high amplitude anomalies are apparent on the Bouguer gravity anomaly map (Figure 3). The map shows two distinguishable areas: a predominant gravity lows trending ENE-WSW, N-S to E-W around the northern area and seeming trending ENE-WSW to E-W gravity highs found in the southern part of the map. Apart from the map which is accentuates the gravimetric values of possibly, definite lithology and structures with the help of colour differences. These variation in colours divide the research area into gravity high (yellow and red colours) and gravity low (green and blue colours).

Regional-residual separation was executed by subtracting upward continued at 5000m on the Bouguer map in order to diminish the effect of the deeply seated structures masking the shallow seated structures. Further qualitative analysis was performed on the residual bouguer map by applying one dimensional Fast Fourier Transform (Figure 4). Consequently, first vertical derivative (Figure 5), first horizontal derivative (Figure 6), upward and

downward continuation at 4000m and 5000m (Figure 7 and 8) maps were generated. The upward continuation process was applied on gravity data of the study area at various levels. The upward continued data reveal increasing attenuation and broadening of the high wave number anomalies with increasing height above the study area. The upward continued map illustrate the change in anomaly character with increasing observation to gravity source distance, and are also helpful as low-wavenumber pass filter. Upward continued data provides excellent integrated view of the study area undistorted by the local, high amplitude, high gradient anomalies of the gravity sources in the shallow portion of the study area. It is apparent that the attenuation of the shallow source anomalies in the upward continuation process permits a clearer or enhanced view of the deeper anomaly source.

The estimated depths from the forward and inverse modelling methods for profiles 1-7 are 3446, 6921, 6182, 5199, 3321, 3152 and 2762m respectively. The respective density values were 0.182, 0.098, 0.043, 0.091, 0.108, 0.079 and 0.079gmcc<sup>-1</sup>, which indicate the presence of sedimentary intrusions (basalt or limestone), few

metamorphic rocks (schist) and minerals (magnetite).

## VI. CONCLUSION

The assessment of the Bouguer gravity datasets shows the existence of E-W, ENE-WSW, WNW- ESE, N-S, NE-SW and NW-SE trending lineaments but with the ENE-WSW and E-W striking trends dominating. The E-W and ENE-WSW tectonic trends are sets of faults induced possibly by gravity tectonics within the study area. From the results obtained, it can be seen that the northwest and northeastern regions of the study area are more prolific and viable for the exploration of mineral resources as well as for further investigations. The regions marked P1, P2, P3, and P6 profiles are suspected of basalt, pyrite, calcite, and limestone should be well targeted for the mineral exploration.

## ACKNOWLEDGEMENTS

We are immensely grateful to the Nigerian Geological Survey Agency (NGSA) for making the datasets available.

## REFERENCES

- [1]. M.B. Dobrin, (1976): Introduction to Geophysical Prospecting 3rd Edition, (McGraw Hill Co, New York 630).
- [2]. J.A. Adekoya, P.S. Ola, and S.O. Olabole, Possible Bornu Basin Hydrocarbon Habitat A reviews. *International Journal of Geosciences*, 5: 2014, 983-996.
- [3]. P.K. Fagbenle, (2016). Hydrocarbon Potentials Prospects in Chad Basin. *Daily Trust News Paper of 25th July*, 9(24), 2016, 4.
- [4]. A.B. Aderoju, S.B. Ojo, A.A. Adepelumi, and F. Edino, (2016). A reassessment of hydrocarbon prospectivity of the Chad Basin, Nigeria, using magnetic hydrocarbon indicators from High – Resolution Aeromagnetic imaging. *Ife Journal of Science*, 18 (2), 2016, 503-520.
- [5]. O. Ajana, E.E. Udensi, M. Momoh, J.K Rai, and S.B. Muhammad, (2014). Spectral Depths Estimatof Subsurface in Parts of Chad Basin Northeastern Nigeria. *Journal of Applied Geology and Geophysics*, 2(2), 2014, 58-6.
- [6]. A.A Avbovbo, E.O. Ayoola, and G.A. Osahon, Depositional and Structural Styles in Chad Basin of Nigeria. *Bulletin American Association Petroleum Geologists*, 70 (121), 1986, 1787-1798.
- [7]. O. Ajana, E.E. Udensi, M. Momoh, J.K. Rai, and S.B. Muhammad, (2014). Spectral Depths Estimatof Subsurface in Parts of Chad Basin Northeastern Nigeria. *Journal of Applied Geology and Geophysics*, 2(2), 2014, 58-6.
- [8]. M.O. Odebode, A handout on geology of Borno (Chad) Basin Northeastern Nigeria. 2010
- [9]. E.A. Okosun, (1995) Review of Borno Basin. *Nigerian Journal of mining and geology*, 31(2), 1995, 113-172.
- [10]. N.G. Obaje, (2009). *Geology and Mineral Resources of Nigeria*, Berlin Springer publishers, 2009.
- [11]. H.S. Zahra, and T.O. Hesham, (2016): Application of high pass filtering techniques on gravity and magnetic data of the eastern Qaltara Depression area, western deseart Egypt. *Nriag journal of Astronomy and Geophysics*, 5, 2016, 106- 123.
- [12]. E.A. Gordon, G. Arthur, Z. Isidore, and F.B. David, *Geologic interpretation of magnetic and gravity data in the copper River basin, Alaska. Geophysical field investigations*, Washington, 316-H, 2006, 135-153.
- [13]. S. Yves, and M.T. Jean, Interpreting gravity anomalies in south Cameroon, central Africa. *Earth Science research journal*, 16, 2012, 5-9.
- [14]. C. Ayala, B. Fernando, M. Adolfo, I.R. María, T. Montserrat, R. Félix, F. Manel, and L.G. José, Updated Bouguer anomalies of the Iberian Peninsula: a new perspective to interpret the regional geology. *Journal of Maps*, 12, 2016, 1089–1092.
- [15]. M.B. Dobrin, and C.H. Savit, *Introduction to geophysical prospecting*. McGraw-Hill books. Pennsylvania Plaza, New York City, U.S.A. 1988.
- [16]. W. Doo, S. Hsu, C. Tsai, and Y. Huang, Using analytic signal to determine magnetization/density ratios of geological structures. *Journal J. International*, 179 (8), 2009.
- [17]. E.A. Gordon, G. Arthur, Z. Isidore, and F.B. David, *Geologic interpretation of magnetic and gravity data in the copper River basin, Alaska. Geophysical field investigations*, Washington, 316, 2006, 135-153.
- [18]. G. Ramadas, D. Himabindu, and I.B Ramaprasada, (2004). Magnetic basement along Jadcharia Vasco transect, Dharwar Craton, India. *Current Science*, 86, (11), 2004, 1548-1553.
- [19]. W.M. Telford, L.P. Geldart, and R.E. Sheriff, *Applied geophysics (2nd edition)*, Cambridge University Press, Cambridge.1990.
- [20]. M.B. Dobrin, and C.H. Savit, *Introduction to geophysical prospecting*. McGraw-Hill books. Pennsylvania Plaza, New York City, U.S.A. 1988.
- [21]. R.E. Sheriff, L.P. Geldart, and W.M. Telford, (1990): *Applied geophysics (2nd edition)*, Cambridge University Press, Cambridge. 1990.